ENOC-2008, Saint Petersburg, Russia, June, 30–July, 4 2008

OPTIMIZATION OF NON-LINEAR MASS DAMPER PARAMETERS FOR TRANSIENT RESPONSE

Jakob S. Jensen
Department of Mechanical Engineering
Nils Koppels Allé, Building 404
Technical University of Denmark
jsj@mek.dtu.dk

Boyan S. Lazarov
Department of Mechanical Engineering
Nils Koppels Allé, Building 404
Technical University of Denmark
bsl@mek.dtu.dk

Abstract
We optimize the parameters of multiple non-linear mass dampers based on numerical simulation of transient wave propagation through a linear mass-spring carrier structure. Topology optimization is used to obtain optimized distributions of damper mass ratio, natural frequency, damping ratio and nonlinear stiffness coefficient. Large improvements in performance is obtained with optimized parameters and it is shown that nonlinear mass dampers can be more effective for wave attenuation than linear mass dampers.

Key words
Non-linear mass dampers, wave propagation, topology optimization.

1 Introduction

In this paper we report on a systematic approach for optimizing the individual parameters of local nonlinear oscillators attached to a linear mass-spring chain. The optimization procedure is based on transient simulation of wave propagation through the linear carrier structure. The work follows a recent theoretical and numerical study (Lazarov and Jensen, 2007) of band gap formation in this non-linear system.

Band gaps are frequency ranges in which waves cannot propagate through the structure (Brillouin, 1953). They occur in infinite periodic systems and also in mass-spring chains with attached oscillators (Liu *et al.*, 2000). In a finite structure excitation with a frequency within the band gap results in a localized response near the point of excitation or at the boundary of the structure (Jensen, 2003). The attached oscillators act as multiple mass dampers (Strasberg and Feit, 1996) that "absorb" waves that propagate in the main chain and can thus be used to reduce the transmission of waves in the chain.

In (Lazarov and Jensen, 2007) it was demonstrated that non-linear oscillators can be used to shift band gap frequencies and control the propagation of waves in the main chain. Additionally, it was demonstrated that a non-uniform distribution of non-linear coefficients could be used to improve the attenuation properties of the structure. In this paper we apply a systematic design procedure based on the method of topology optimization (Bendsøe and Sigmund, 2003) to find optimized sets of oscillators parameters that minimize the transmission of waves.

The paper is organized as follows. In Section 2 we introduce the physical and numerical model. Typical transient behavior is illustrated in Section 3. Section 4 presents the optimization algorithm including sensitivity analysis. In Section 5 we show examples of optimized oscillator parameters for mono-frequency steady-state behavior as well as full transient behavior. In Section 6 we give conclusions.

2 A mass-spring chain with attached nonlinear oscillators

Fig. 1 illustrates the basic unit cell. The coupled equations for the displacement of a mass in the chain, denoted u_j, and the displacement of the attached oscillator read:

$$\ddot{u}_j + 2u_j - u_{j-1} - u_{j+1} = \beta(\omega^2 q + \gamma q^3 + 2\zeta\omega\dot{q}) \quad (1)$$

$$\ddot{q} + 2\zeta\omega\dot{q} + \omega^2 q + \gamma q^3 = -\ddot{u}_j \quad (2)$$

Non-dimensional parameters in (1)–(2) are $\beta = M/m$ which is the ratio between the mass of the oscillator and the mass to which it is attached, ω is the natural frequency of the oscillator relative to a characteristic frequency of the main chain denoted $\omega_0 = \sqrt{k/m}$, ζ is the damping ratio of the oscillator and γ is the non-linear stiffness coefficient. Additionally, the non-dimensional time measure $\tau = \omega_0 t$ has been introduced.

We consider a finite system based on the building block unit cell in Fig. 1. Fig. 2 shows this finite system.

The number of masses in the chain that carry an oscillator is denoted N. Additionally, a number of masses without attached oscillators are connected to the chain at both ends; N_{in} to the left, and N_{out} to the right of the section with oscillators. All oscillators may have different parameters, denoted β_i, ω_i, γ_i and ζ_i, whereas the main chain consist of equal springs with stiffness k and equal masses m. By setting both end masses to $m/2$ and adding viscous dampers ($c = \sqrt{mk}$) we mimic transparent boundaries at both ends of the chain.

Wave motion is imposed by a time-dependent force $f(t)$ acting on the leftmost mass in the chain. The specific force is to be specified in the forthcoming example sections.

Eqs. (1)–(2) are rewritten in matrix form. We introduce a vector of the unknown displacements:

$$\mathbf{u} = \{u_1\ u_2\ \ldots\ u_{N+N_{\text{in}}+N_{\text{out}}}\ q_1\ q_2\ \ldots\ q_N\}^T \quad (3)$$

and can write the model equations as:

$$\ddot{\mathbf{u}} + \mathbf{C}\dot{\mathbf{u}} + \mathbf{K}\mathbf{u} + \mathbf{F}_{\text{non}}(\mathbf{u}) = \mathbf{F}_{\text{ext}} \quad (4)$$

In (4) $\mathbf{C}$ is a damping matrix, $\mathbf{K}$ is a stiffness matrix, $\mathbf{F}_{\text{non}}$ is a vector of nonlinear forces and the vector $\mathbf{F}_{\text{ext}}$ contains the external load.

3 Numerical simulation of system behavior

The optimization algorithm is based on repeated analyses of (4), sometimes several hundred, thus a fast and robust numerical solver is essential. We use a central-difference explicit scheme (Cook *et al.*, 2002) that is very fast and stable with a sufficiently small time step.

In all numerical simulations we use trivial initial conditions $\mathbf{u} = \dot{\mathbf{u}} = \mathbf{0}$ and the total simulation time is denoted $\mathcal{T}$.

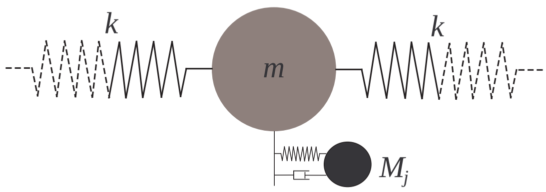

Figure 1. Basic unit cell with a mass in the linear main chain and an attached non-linear oscillator.

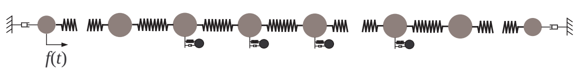

Figure 2. Finite chain consisting of N masses with attached oscillators, N_{in} and N_{out} masses without oscillators in the left and right end. Viscous dampers are added in the ends to simulate transparent boundaries.

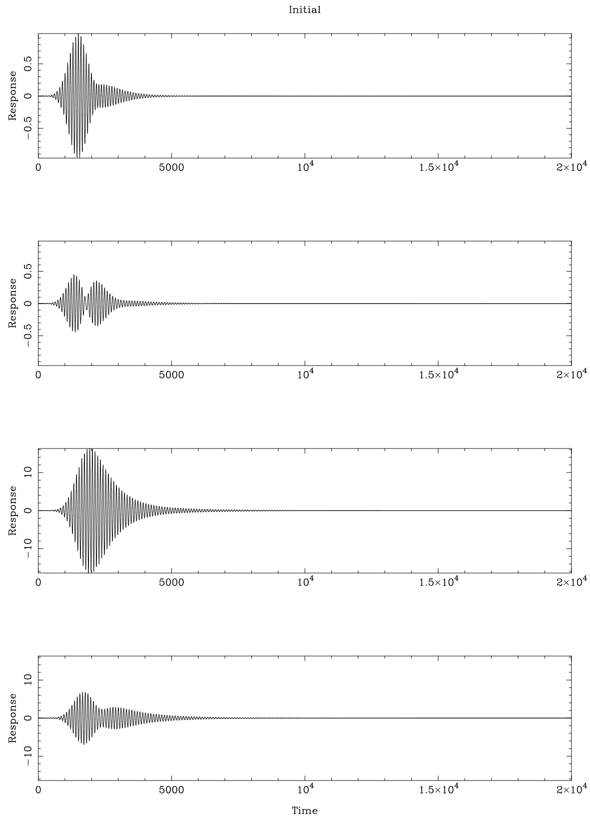

Figure 3. Typical transient response. Figures shows (from top and down): Response of the leftmost and rightmost mass in the main chain, response of the first and last attached oscillator.

Fig. 3 shows typical simulation results for transient response of the system – here for the following set of system parameters:

$\beta = 0.1, \zeta = 0.01, \omega = \Omega = 0.0625, \gamma = 0$
$N = 26, N_{\text{in}} = N_{\text{out}} = 1$
$f(t) = \sin(\Omega(t - t_0))e^{-\delta(t-t_0)^2}$
$t_0 = 1500, \delta = 0.000004$

In Fig. 3 the response of the rightmost mass in the chain is depicted (second plot from top). This illustrates the signal actually transmitted through the chain. It is seen that the transmitted signal is composed of a main signal transmitted instantly followed by a trailing signal due to reflections in the structure.

4 Optimization of mass damper parameters

We will in the following quantify the mass damper performance by considering the response of the rightmost mass in the chain integrated over a certain time interval. We consider the general objective function:

$$\Phi = \int_{\mathcal{T}_1}^{\mathcal{T}_2} c(\mathbf{u})dt \quad (5)$$

in which $c(\mathbf{u})$ is a positive real function of the displacement vector. The smaller Φ is, the more effective the attached mass dampers.

We wish to minimize the functional Φ by manipulating the parameters of each of the N attached oscillators. We may vary all 4 parameters β_i, ω_i, γ_i and ζ_i and have in total $4 \times N$ design variables which are defined by the following relations:

$$\beta_i = \beta_{\min} + x_i^\beta(\beta_{\max} - \beta_{\min}) \tag{6}$$
$$\omega_i = \omega_{\min} + x_i^\omega(\omega_{\max} - \omega_{\min}) \tag{7}$$
$$\gamma_i = \gamma_{\min} + x_i^\gamma(\gamma_{\max} - \gamma_{\min}) \tag{8}$$
$$\zeta_i = \zeta_{\min} + x_i^\zeta(\zeta_{\max} - \zeta_{\min}) \tag{9}$$

in which the subscript min and max refer to upper and lower bounds on the parameters that are specified *a priori*. Thus, continuous design variables varying between 0 and 1 let the material parameters take any value between these min and max values.

A higher mass of the oscillators generally leads to increased wave attenuation. In order to give a fair comparison between the performance of different structures we therefore introduce a limit on the maximum average mass ratio $\tilde{\beta}$, such that:

$$\tfrac{1}{N}\sum_{i=1}^{N}\beta_i < \tilde{\beta} \tag{10}$$

The continuous design variables allow us to apply a gradient-based optimization algorithm to optimize the performance of the structure. In order to do this we need to compute the gradient of Φ with respect to x_i^β, x_i^ω, x_i^γ and x_i^ζ. Let x denote any design variable, then by using the chain rule we obtain:

$$\frac{\mathrm{d}\Phi}{\mathrm{d}x} = \int_{\mathcal{T}_1}^{\mathcal{T}_2} \frac{\mathrm{d}c}{\mathrm{d}\mathbf{u}}\frac{\mathrm{d}\mathbf{u}}{\mathrm{d}x}dt = \int_0^{\mathcal{T}_2} \frac{\mathrm{d}c}{\mathrm{d}\mathbf{u}}\frac{\mathrm{d}\mathbf{u}}{\mathrm{d}x}dt - \int_0^{\mathcal{T}_1} \frac{\mathrm{d}c}{\mathrm{d}\mathbf{u}}\frac{\mathrm{d}\mathbf{u}}{\mathrm{d}x}dt \tag{11}$$

In order to eliminate the term $\frac{\mathrm{d}\mathbf{u}}{\mathrm{d}x}$ we use the adjoint method that has previously been applied to transient design problems (Bendsøe and Sigmund, 2003). We rewrite (11) as:

$$\frac{\mathrm{d}\Phi}{\mathrm{d}x} = \int_0^{\mathcal{T}_2} (\frac{\mathrm{d}c}{\mathrm{d}\mathbf{u}}\frac{\mathrm{d}\mathbf{u}}{\mathrm{d}x} + \boldsymbol{\lambda}_1^T\frac{\mathrm{d}\mathbf{R}}{\mathrm{d}x})dt - \int_0^{\mathcal{T}_1} (\frac{\mathrm{d}c}{\mathrm{d}\mathbf{u}}\frac{\mathrm{d}\mathbf{u}}{\mathrm{d}x} + \boldsymbol{\lambda}_2^T\frac{\mathrm{d}\mathbf{R}}{\mathrm{d}x})dt \tag{12}$$

in which

$$\mathbf{R} = \ddot{\mathbf{u}} + \mathbf{C}\dot{\mathbf{u}} + \mathbf{K}\mathbf{u} + \mathbf{F}_{\text{non}}(\mathbf{u}) - \mathbf{F}_{\text{ext}} \tag{13}$$

is the residual that vanishes at equilibrium.

We compute

$$\frac{\mathrm{d}\mathbf{R}}{\mathrm{d}x} = \frac{\mathrm{d}\ddot{\mathbf{u}}}{\mathrm{d}x} + \frac{\mathrm{d}\mathbf{C}}{\mathrm{d}x}\ddot{\mathbf{u}} + \mathbf{C}\frac{\mathrm{d}\dot{\mathbf{u}}}{\mathrm{d}x} + \frac{\mathrm{d}\mathbf{K}}{\mathrm{d}x}\mathbf{u} + \mathbf{K}\frac{\mathrm{d}\mathbf{u}}{\mathrm{d}x} + \frac{\mathrm{d}\mathbf{F}_{\text{non}}}{\mathrm{d}x} + \frac{\mathrm{d}\mathbf{F}_{\text{non}}}{\mathrm{d}\mathbf{u}}\frac{\mathrm{d}\mathbf{u}}{\mathrm{d}x} \tag{14}$$

since we assume that the external force (wave input) is independent of the design. By inserting (14) and performing partial integration we rewrite (12) into:

$$\begin{aligned}\frac{\mathrm{d}\Phi}{\mathrm{d}x} &= \int_0^{\mathcal{T}_2}\Big((\frac{\mathrm{d}c}{\mathrm{d}\mathbf{u}} + \ddot{\boldsymbol{\lambda}}_1^T - \dot{\boldsymbol{\lambda}}_1^T\mathbf{C} + \boldsymbol{\lambda}_1^T(\mathbf{K} + \frac{\mathrm{d}\mathbf{F}_{\text{non}}}{\mathrm{d}\mathbf{u}}))\frac{\mathrm{d}\mathbf{u}}{\mathrm{d}x} + \boldsymbol{\lambda}_1^T(\frac{\mathrm{d}\mathbf{C}}{\mathrm{d}x}\ddot{\mathbf{u}} + \frac{\mathrm{d}\mathbf{K}}{\mathrm{d}x}\mathbf{u} + \frac{\mathrm{d}\mathbf{F}_{\text{non}}}{\mathrm{d}x})\Big)dt \\ &- \int_0^{\mathcal{T}_1}\Big((\frac{\mathrm{d}c}{\mathrm{d}\mathbf{u}} + \ddot{\boldsymbol{\lambda}}_2^T - \dot{\boldsymbol{\lambda}}_2^T\mathbf{C} + \boldsymbol{\lambda}_2^T(\mathbf{K} + \frac{\mathrm{d}\mathbf{F}_{\text{non}}}{\mathrm{d}\mathbf{u}}))\frac{\mathrm{d}\mathbf{u}}{\mathrm{d}x} + \boldsymbol{\lambda}_2^T(\frac{\mathrm{d}\mathbf{C}}{\mathrm{d}x}\ddot{\mathbf{u}} + \frac{\mathrm{d}\mathbf{K}}{\mathrm{d}x}\mathbf{u} + \frac{\mathrm{d}\mathbf{F}_{\text{non}}}{\mathrm{d}x})\Big)dt \\ &+ \Big[\boldsymbol{\lambda}_1^T\mathbf{C}\frac{\mathrm{d}\mathbf{u}}{\mathrm{d}x} + \boldsymbol{\lambda}_1^T\frac{\mathrm{d}\dot{\mathbf{u}}}{\mathrm{d}x} - \dot{\boldsymbol{\lambda}}_1^T\frac{\mathrm{d}\mathbf{u}}{\mathrm{d}x}\Big]_0^{\mathcal{T}_2} - \Big[\boldsymbol{\lambda}_2^T\mathbf{C}\frac{\mathrm{d}\mathbf{u}}{\mathrm{d}x} + \boldsymbol{\lambda}_2^T\frac{\mathrm{d}\dot{\mathbf{u}}}{\mathrm{d}x} - \dot{\boldsymbol{\lambda}}_2^T\frac{\mathrm{d}\mathbf{u}}{\mathrm{d}x}\Big]_0^{\mathcal{T}_1}\end{aligned} \tag{15}$$

By choosing the following conditions:

$$\boldsymbol{\lambda}_1(\mathcal{T}_2) = \dot{\boldsymbol{\lambda}}_1(\mathcal{T}_2) = 0 \tag{16}$$
$$\boldsymbol{\lambda}_2(\mathcal{T}_1) = \dot{\boldsymbol{\lambda}}_2(\mathcal{T}_1) = 0 \tag{17}$$

and by requiring the initial response of the structure to be independent of the design the terms in the square brackets vanish.

We now require the terms inside the integration terms that are coefficients to $\frac{\mathrm{d}\mathbf{u}}{\mathrm{d}x}$ to vanish:

$$\ddot{\boldsymbol{\lambda}}_1^T - \dot{\boldsymbol{\lambda}}_1^T\mathbf{C} + \boldsymbol{\lambda}_1^T(\mathbf{K} + \frac{\mathrm{d}\mathbf{F}_{\text{non}}}{\mathrm{d}\mathbf{u}}) = -\frac{\mathrm{d}c}{\mathrm{d}\mathbf{u}} \tag{18}$$
$$\ddot{\boldsymbol{\lambda}}_2^T - \dot{\boldsymbol{\lambda}}_2^T\mathbf{C} + \boldsymbol{\lambda}_2^T(\mathbf{K} + \frac{\mathrm{d}\mathbf{F}_{\text{non}}}{\mathrm{d}\mathbf{u}}) = -\frac{\mathrm{d}c}{\mathrm{d}\mathbf{u}} \tag{19}$$

These two new transient problems are solved for $\boldsymbol{\lambda}_1$ and $\boldsymbol{\lambda}_1$ and we can compute the sensitivities by the final expression:

$$\frac{\mathrm{d}\Phi}{\mathrm{d}x} = \int_0^{\mathcal{T}_2}\boldsymbol{\lambda}_1^T(\frac{\mathrm{d}\mathbf{C}}{\mathrm{d}x}\ddot{\mathbf{u}} + \frac{\mathrm{d}\mathbf{K}}{\mathrm{d}x}\mathbf{u} + \frac{\mathrm{d}\mathbf{F}_{\text{non}}}{\mathrm{d}x})dt - \int_0^{\mathcal{T}_1}\boldsymbol{\lambda}_2^T(\frac{\mathrm{d}\mathbf{C}}{\mathrm{d}x}\ddot{\mathbf{u}} + \frac{\mathrm{d}\mathbf{K}}{\mathrm{d}x}\mathbf{u} + \frac{\mathrm{d}\mathbf{F}_{\text{non}}}{\mathrm{d}x})dt \tag{20}$$

Our strategy for optimizing the oscillator parameters can be summarized as: perform repeated analyses of (4), with each analysis followed by a computation of the sensitivities by solving (18), (19) and (20), and the sensitivities provided to a mathematical programming software MMA (Svanberg, 1987) to obtain a design update. This iterative procedure is continued until design converges within a specified threshold.

5 Results

The optimization algorithm is demonstrated by two examples where we consider steady-state and transient response. In both examples we find optimized sets of oscillator parameters that minimize the transmitted wave.

5.1 Steady-state mono-frequency behavior

As the first example we optimize the system parameters for mono-frequency steady-state behavior. The system parameters and excitation is:

$$N = 26, N_{\text{in}} = N_{\text{out}} = 1, \Omega = 0.0625$$
$$f(t) = \sin(\Omega(t - t_0))e^{-\delta(t-t_0)^2},\ t < t_0$$
$$f(t) = \sin(\Omega(t - t_0)),\ t > t_0$$
$$t_0 = 2500, \delta = 0.000002$$

and the objective function is evaluated in the time interval specified by $\mathcal{T}_1 = 15000$ and $\mathcal{T}_2 = 20000$. In this way we ensure that the response has reached steady state.

First we consider linear oscillators ($\gamma_i = 0$) and optimize the distribution of natural frequencies and mass ratios. The damping ratio is fixed at $\zeta = 0.01$. We allow the parameters to vary as follows:

$$\omega_{\min} = 0.0615, \omega_{\max} = 0.0630$$
$$\beta_{\min} = 0.0, \beta_{\max} = 0.2$$

and keep the maximum average mass ratio at $\tilde{\beta} = 0.1$. Fig. 4 shows the oscillator parameters for the optimized design and Fig. 5 displays the response of the leftmost and rightmost mass in the chain (two top plots) as well as the response of the first and last oscillator (two bottom plots). An almost uniform distribution of natural frequencies is obtained, close to the excitation frequency. This is expected for mono-frequency excitation (cf. working principles of standard mass dampers). The slight detuning between the excitation and natural frequencies is due to the presence of damping. The optimized design is composed mainly of oscillators with the maximum mass ratio ($\beta = 0.2$) and minimum mass ratio ($\beta = 0$ - corresponding to no oscillator). A physical interpretation of the effects of this mass distribution is difficult due to the complexity of the wave motion, but the effect is a reduction of the objective with about 22% compared to an optimized design with a fixed uniform mass ratio of $\beta = 0.1$.

If we allow the non-linear stiffness coefficients to vary the performance of the mass dampers can be further improved. The minimum and maximum coefficients are chosen as:

$$\gamma_{\min} = -0.00006, \gamma_{\max} = 0.00006$$

As seen in Fig. 6 the the distribution of natural frequencies and mass ratios is qualitatively similar to the linear case. However, the distribution is no longer symmetric around the chain center and more irregular. The natural frequencies are lower than for the linear case but this is combined with positive (hardening) non-linear

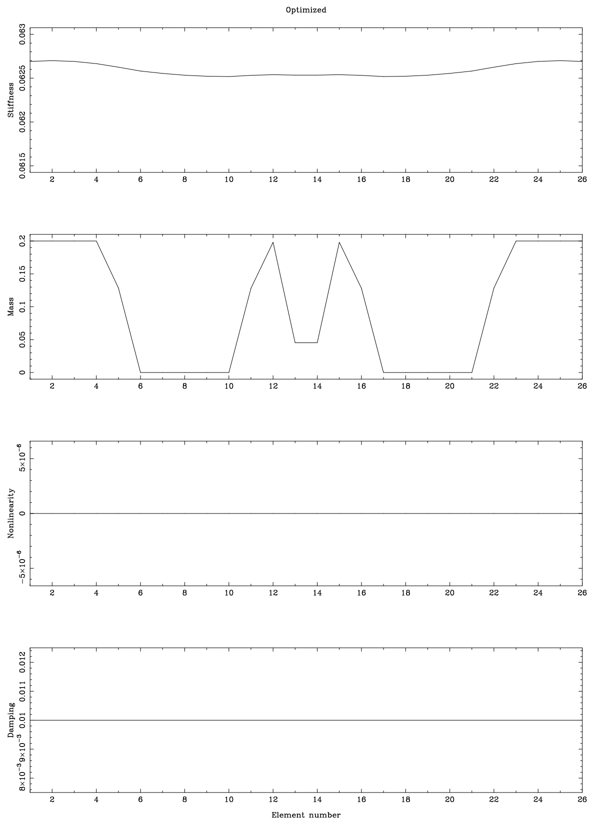

Figure 4. Optimized distribution of natural frequencies and mass ratios for steady-state response. Zero nonlinearity and uniform damping ratio.

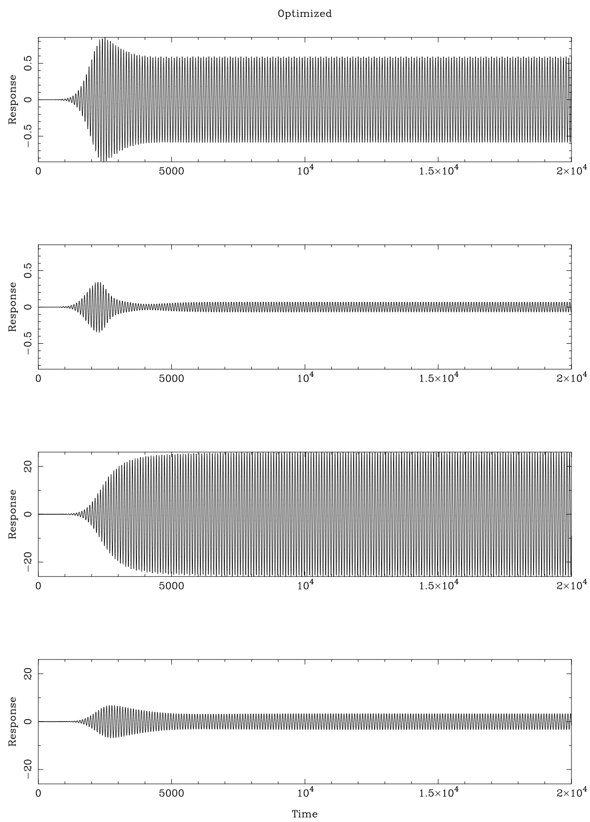

Figure 5. Response for optimized design shown in Fig. 4.

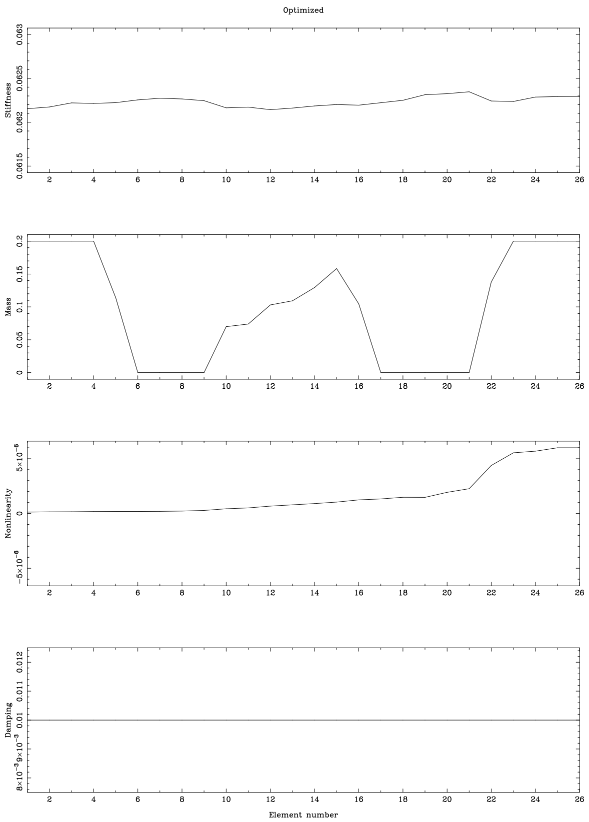

Figure 6. Optimized distribution of natural frequencies, mass ratios and non-linear coefficients for steady-state response. Uniform damping ratio.

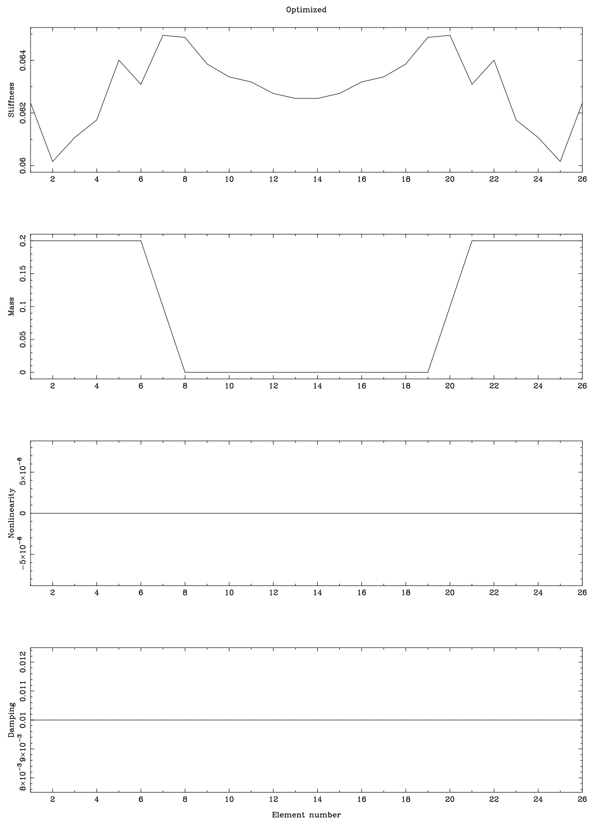

Figure 8. Optimized distribution of natural frequencies and mass ratios for transient response. Zero nonlinearity and uniform damping ratio.

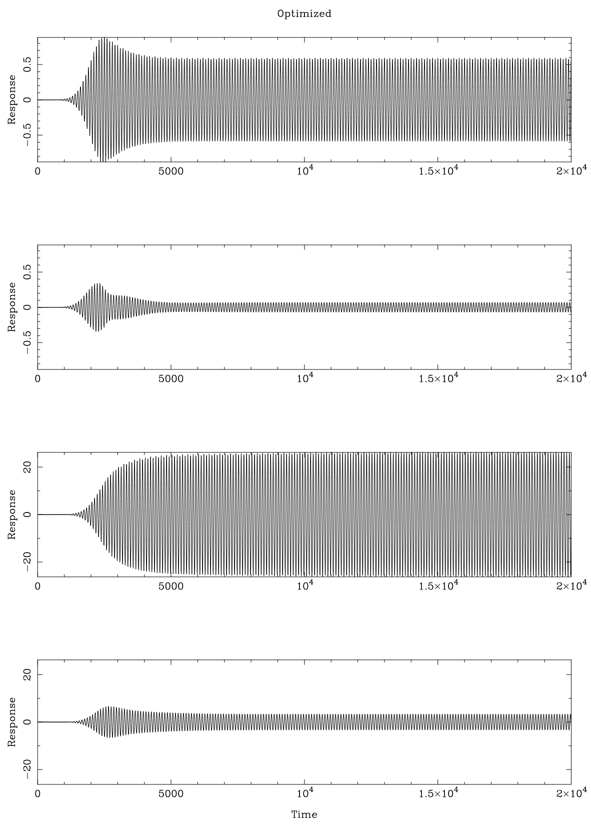

Figure 7. Response for optimized design shown in Fig. 6.

stiffness that increases along the chain length. The objective function is reduced by 2.4% compared to the linear case.

It should be noted that a reduction of the damping ratio ζ always cause a further reduction of Φ. No beneficial effects of a non-uniform damping distribution has been observed.

5.2 Transient response

We now consider the full transient response of the chain. The system parameters and excitation are:

$$N = 26, N_{\text{in}} = N_{\text{out}} = 1, \Omega = 0.0625$$
$$f(t) = \sin(\Omega(t - t_0))e^{-\delta(t-t_0)^2}$$
$$t_0 = 2500, \delta = 0.000002$$

and the objective function evaluates the response in the entire simulation time interval: $\mathcal{T}_1 = 0$ and $\mathcal{T}_2 = 20000$.

Fig. 8 shows the optimized design with zero nonlinearity and uniform damping ratio $\zeta = 0.01$. The minimum and maximum values of the natural frequency and mass ratio are:

$$\omega_{\text{min}} = 0.060, \omega_{\text{max}} = 0.064$$
$$\beta_{\text{min}} = 0.0, \beta_{\text{max}} = 0.2$$

with a constraint on the average mass ratio of $\tilde{\beta} = 0.1$.

Fig. 8 shows a larger variation of the natural frequen-

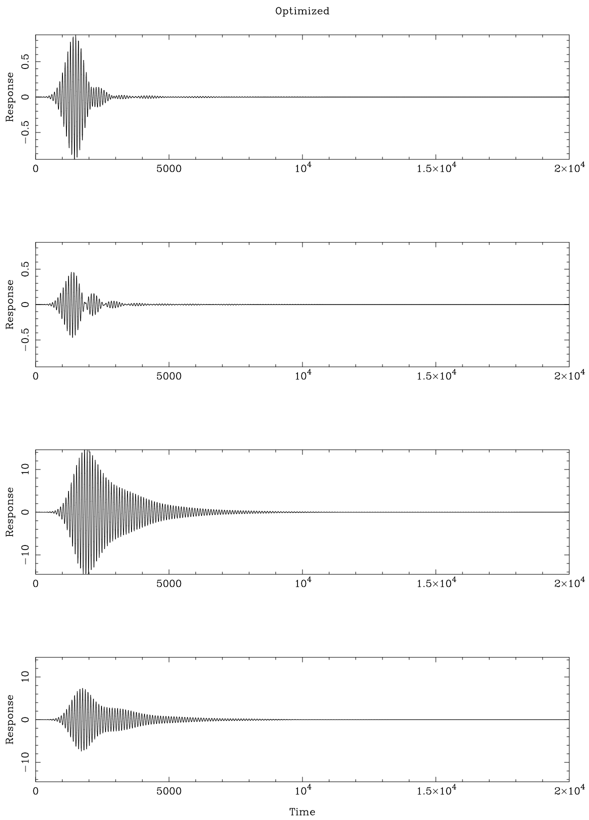

Figure 9. Response for optimized design shown in Fig. 8.

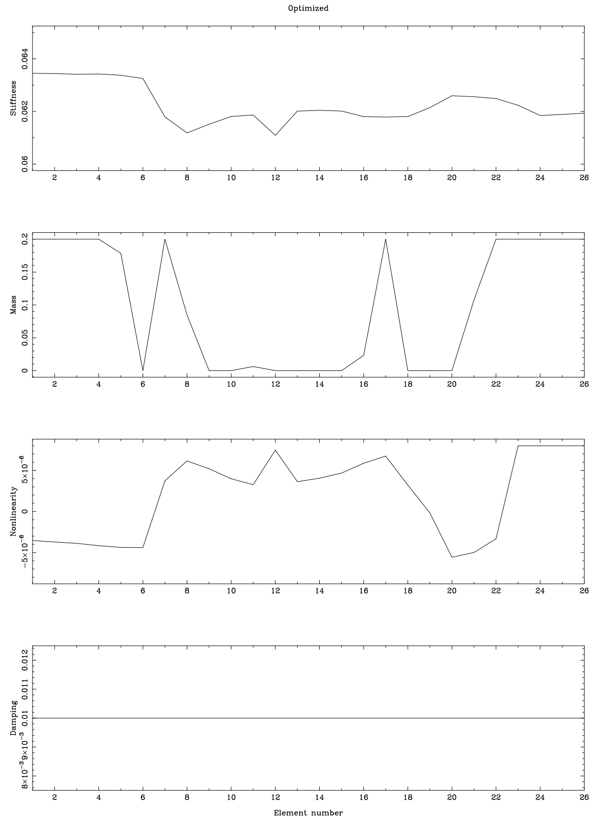

Figure 10. Optimized distribution of natural frequencies, mass ratios and non-linear coefficients for transient response. Zero nonlinearity and uniform damping ratio.

cies than for the steady-state case. This is a results of the broader frequency content of the wave pulse, and thus a broader spectrum of oscillator frequencies are needed to quench the signal effectively. The response shown in Fig. 9 reveals that the output signal consists of a main signal followed by smaller trailing pulses.

We now allow the nonlinear stiffness to vary between:

$$\gamma_{\min} = -0.00006, \gamma_{\max} = 0.00006$$

Interestingly, the $\gamma-$distribution shows alternating sections of softening and hardening non-linearities in the optimized design. This is combined with an irregular $\omega-$distribution. As a result the trailing pulses in the output signal (Fig. 11) are now significantly reduced in magnitude, leading to a further reduction of the objective function by 21%. Thus, adding nonlinearities allow for a significant extra reduction of the transmission of a pulse, whereas for the steady-state response the effect was smaller.

6 Conclusion

We have used topology optimization based on transient simulation to design the individual parameters of nonlinear oscillators attached to linear mass-spring chain. The optimized parameters minimize the transmission of wave pulses through the main chain.

The natural frequency, mass ratio, nonlinear stiffness and damping ratio of each oscillator were optimized.

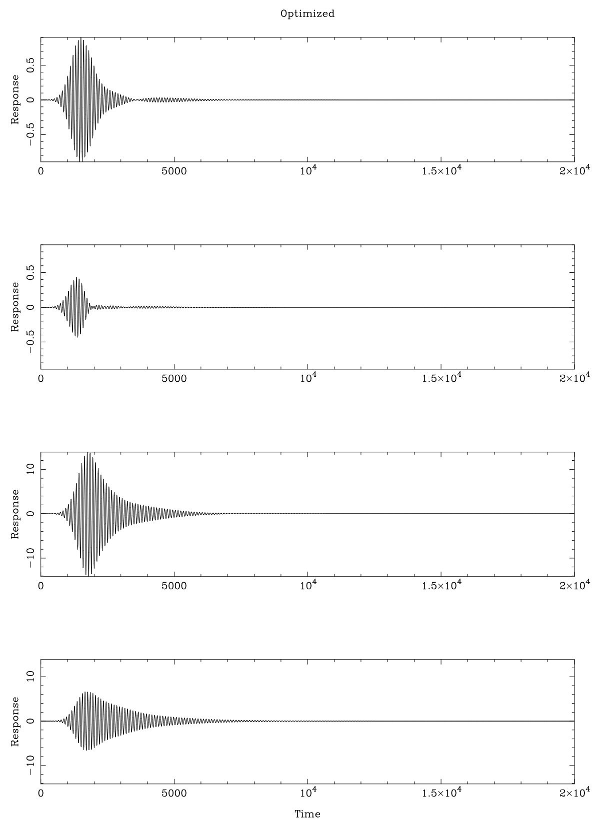

Figure 11. Response for optimized design shown in Fig. 10.

Non-trivial parameter distributions were obtained leading to a significant reduction of the transmitted wave signal. Two examples were considered. For a mono-frequency steady-state response it was noted that a hardening but non-uniform nonlinearity was favored whereas for a full transient simulation combinations of softening and hardening nonlinearities appeared in the optimized design. It was shown also that including non-linear stiffness was beneficial compared to having only a linear oscillator. This was most pronounced for when considering the full transient response.

Acknowledgement

This work was supported by grant 274-05-0498 from the Danish Research Council for Technology and Production Sciences.

References

Bendsøe, M. P. and O. Sigmund (2003). *Topology Optimization - Theory, Methods and Applications*. Springer Verlag, Berlin Heidelberg.

Brillouin, L. (1953). *Wave propagation in periodic structures*. 2 ed.. Dover Publications.

Cook, R. D., D. S. Malkus, M. E. Plesha and R. J. Witt (2002). *Concepts and applications of finite element analysis, 4th Ed.*. Wiley, New York.

Jensen, J. S. (2003). Phononic band gaps and vibrations in one- and two-dimensional mass-spring structures. *Journal of Sound and Vibration* **266**(5), 1053–1078.

Lazarov, B. S. and J. S. Jensen (2007). Low-frequency band gaps in chains with attached non-linear oscillators. *International Journal of Non-Linear Mechanics* **42**(10), 1186–1193.

Liu, Z., X. Zhang, Y. Mao, Y. Y. Zhu, Z. Yang, C. T. Chan and P. Sheng (2000). Locally resonant sonic materials. *Science* **289**, 1734–1736.

Strasberg, M. and D. Feit (1996). Vibration damping of large structures induced by attached small resonant structures. *Journal of the Acoustical Society of America* **99**(1), 335–344.

Svanberg, K. (1987). The method of moving asymptotes - a new method for structural optimization. *International Journal for Numerical Methods in Engineering* **24**, 359–373.